patients with NSCLC over a long term. TYMS activity is necessary for cell proliferation because it catalyses an essential step in DNA synthesis, while its overexpression is reported to be associated with tumor proliferation, as well as poor prognosis, in a variety of cancer types (11, 12). As shown in Table IIIB, multivariate analysis revealed that a high level of *TYMS* mRNA was independently correlated to overall survival with a high hazard ratio, indicating that this marker can precisely perform prognosis for patients with lung AD. Determination of gene expression by RT-PCR is a useful technique for small-sized specimens, thus quantification of *TYMS* mRNA levels is clinically sensitive and useful for determining the prognosis of AD patients (7).

As DPD is a rate-limiting enzyme in the catabolism of 5-FU, its high expression in tumors is reported to result in a low sensitivity to 5-FU therapy (13). In the present study, we evaluated the efficacy of 5-FU administration as adjuvant chemotherapy, in relation to intratumoral *DPD* mRNA levels in lung AD patients. Our results revealed that *DPD* expression was significantly inversely correlated to the overall survival of patients administered 5-FU following surgery, indicating that patients with low levels of *DPD* expression in cancer tissue are sensitive to 5-FU. Furthermore, for patients with low DPD-expressing tumors, those administered 5-FU had a significantly better prognosis than those who underwent surgery alone. These findings suggest that the intratumoral *DPD* mRNA level is a possible predictor for the efficacy of 5-FU administration after surgery in lung AD patients. Interestingly, in patients with high DPD-expressing tumors, those administered 5-FU had a tendency for worse prognosis than those who underwent surgery alone (Figure 3B), suggesting that 5-FU may not have benefits for patients with high DPD-expressing tumors. Multivariate analysis showed that administration of 5-FU was an independent variable predicting prognosis of patients with low DPD-expressing lung ADs. Based on these results, determination of *DPD* mRNA levels in lung AD tumors may provide important information for clinicians to decide whether or not to proceed with 5-FU-based chemotherapy for their patients.

Based on our findings for biomarkers associated with 5-FU therapy, it is considered important to evaluate the expressions of TYMS and DPD before establishing a protocol for made-to-order chemotherapy for NSCLC patients (14). In addition, investigation of the effects of more aggressive adjuvant therapy for patients with NSCLC who have elevated *TYMS* or *DPD* mRNA levels is also necessary. Takizawa *et al*. reported that *in vitro* sensitivity to platinum-derived drugs, such as cisplatin and carboplatin, was associated with the expression of *TYMS* and *DPD* in NSCLC specimens (15). They hypothesized that these may be novel markers of DNA repair capacity and may also be linked with chemosensitivity to drugs other than 5-FU. Furthermore, it is important to clarify the roles of TYMS and DPD in regards to chemosensitivity toward various chemotherapy regimens, as their inhibition is now receiving attention for new cancer treatment drugs development. Recently, S-1, a combination of tegafur, gimeracil, and oteracil potassium (Taiho Pharmaceutical), was developed for clinical use (4). Gimeracil is a stronger inhibitor of DPD than uracil when used with UFT. However, Takeda *et al*. reported that a high level of DPD expression predicted resistance to S-1-based chemotherapy in patients with advanced NSCLC (16). Therefore, additional investigations of the effects of new

Table III.

A. Univariate analysis of overall survival in all patients.

Factors	Hazard ratio	95% CI	*p*-Value
Tumor status			
pT3 *vs.* pT1	3.71	1.05-13.2	0.042
pT2 *vs.* pT1	1.91	0.93-3.90	0.079
Nodal status			
pN2 *vs.* pN0	3.33	1.54-7.21	0.002
pN1 *vs.* pN0	1.73	0.67-4.45	0.259
TYMS mRNA			
High *vs.* low	4.17	1.81-9.03	0.001
DPD mRNA			
High *vs.* low	1.09	0.55-2.520	0.804
Administration			
5-FU *vs.* none	1.46	0.68-3.15	0.337

B. Multivariate analysis of overall survival in all patients.

Factor	Hazard ratio	95% CI	*p*-Value
Tumor status			
pT3 *vs.* pT1	2.51	0.69-9.12	0.161
pT2 *vs.* pT1	1.27	0.59-2.75	0.546
Nodal status			
pN2 *vs.* pN0	2.56	1.16-5.66	0.020
pN1 *vs.* pN0	1.41	0.51-3.87	0.511
TYMS mRNA			
High *vs.* low	3.42	1.46-8.02	0.005

C. Multivariate analysis of overall survival in patients with low DPD-expressing tumors.

Factor	Hazard ratio	95% CI	*p*-Value
Nodal status			
pN2 *vs.* pN0	1.42	0.42-4.76	0.570
pN1 *vs.* pN0	0.85	0.22-3.27	0.816
TYMS mRNA			
High *vs.* low	5.31	1.17-24.0	0.030
Administration			
5-FU *vs.* none	7.60	1.02-56.7	0.050

CI, Confidence interval. TYMS, Thymidylate synthase. DPD, Dihydropyrimidine dehydrogenase. 5-FU, 5-fluorouracil.

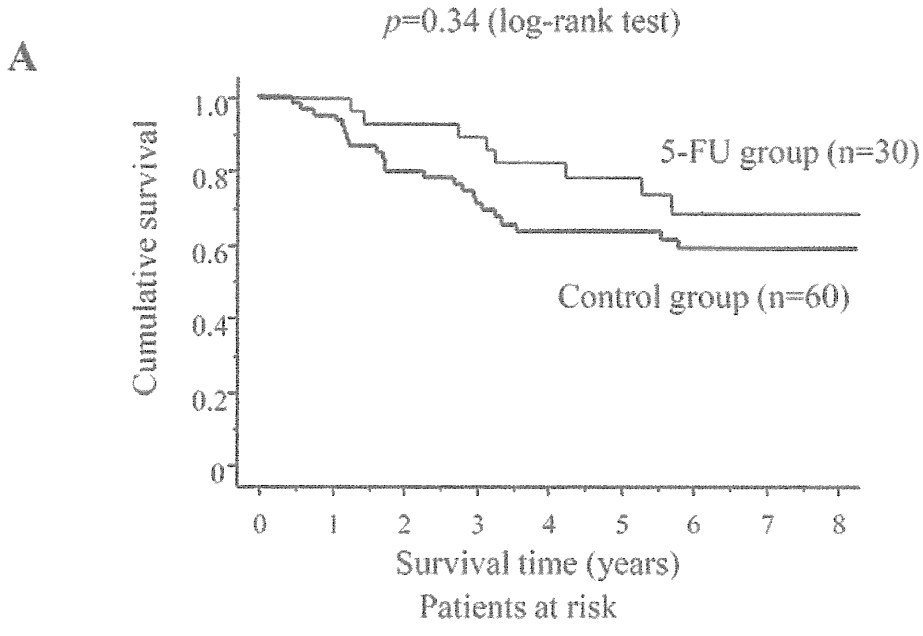

Patients at risk

Control	60	47	32	24	12
5-FU	30	27	22	12	6

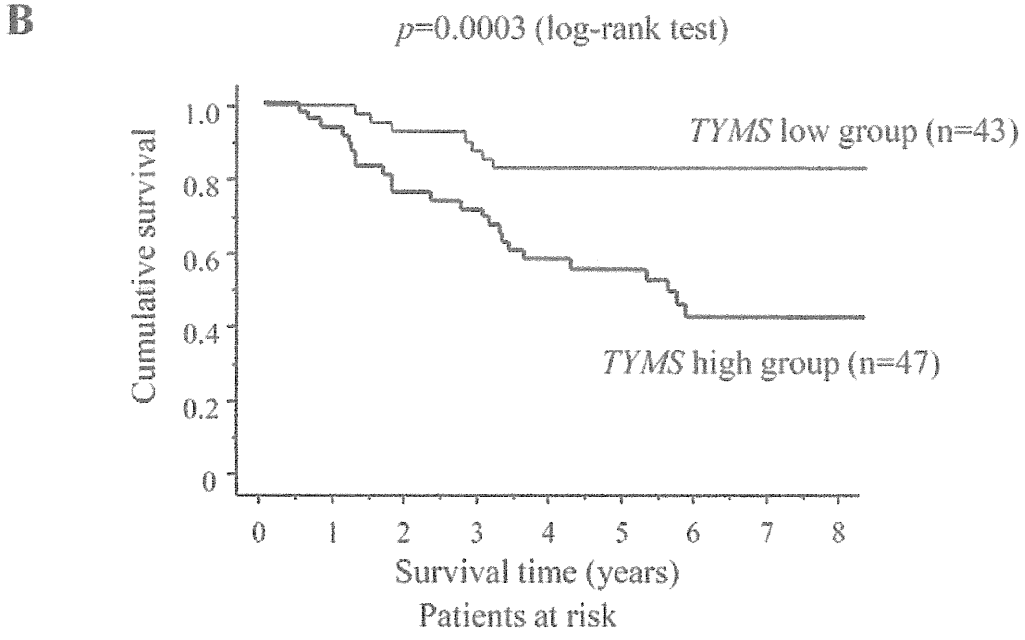

Patients at risk

TYMS high	47	35	23	13	8
TYMS low	43	39	31	23	10

Figure 1. *A: Overall survival curves for patients administered and those not administered 5-fluorouracil (5-FU) after surgery. B: Overall survival curves for patients with high and low thymidylate synthase (TYMS) mRNA levels in resected cancer tissues when dichotomized at the mean TYMS mRNA level.*

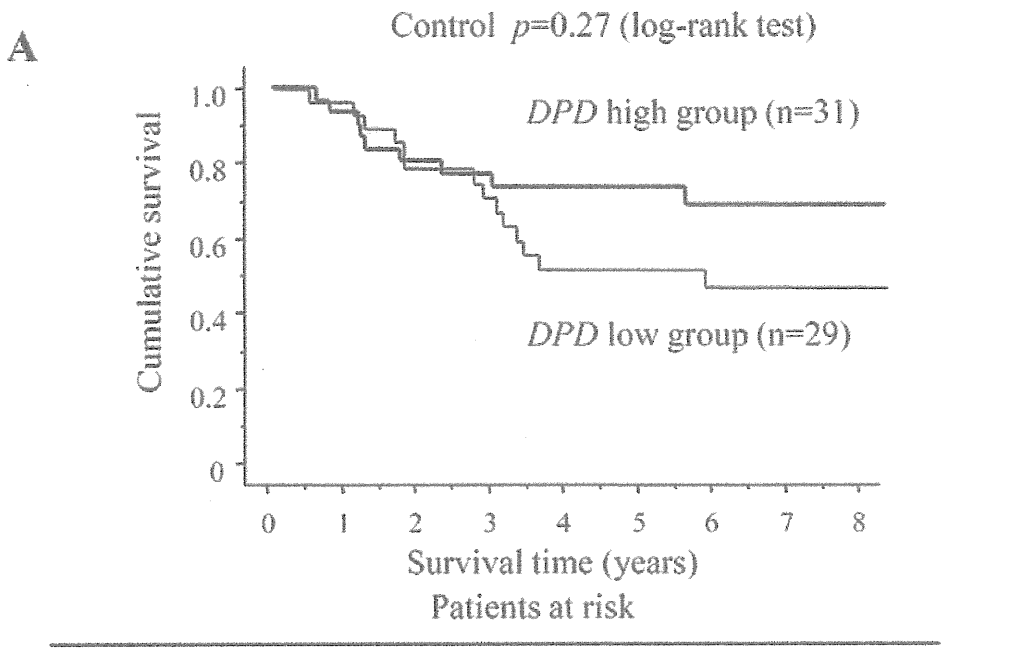

Patients at risk

DPD high	31	25	19	14	7
DPD low	29	22	13	10	5

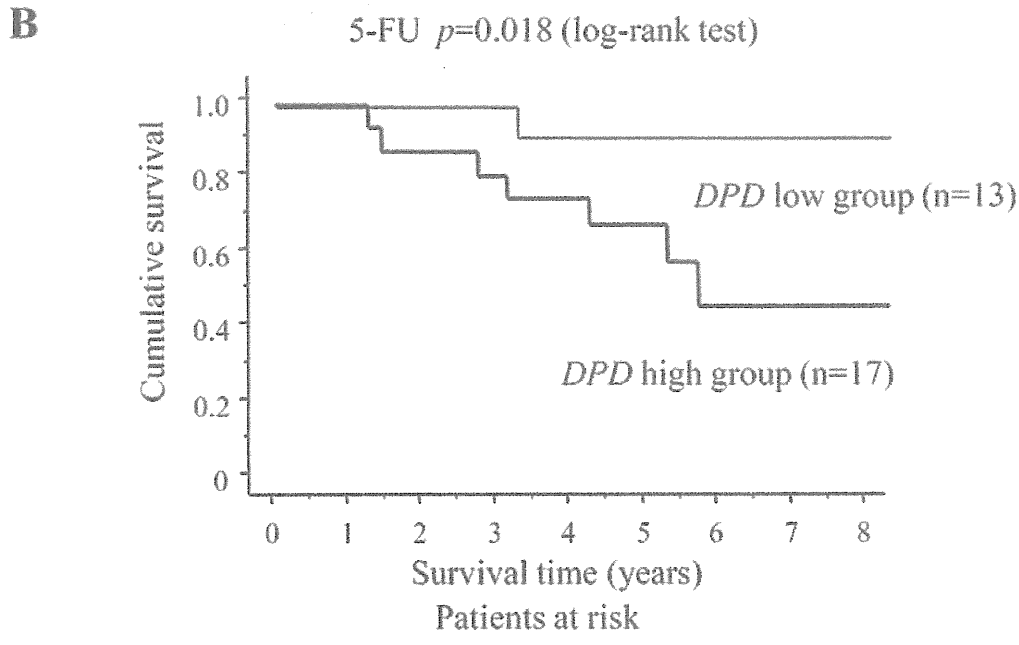

Patients at risk

DPD high	17	14	11	3	2
DPD low	13	13	11	9	4

Figure 2. *A: Overall survival curves for patients with low and high dihydropyrimidine dehydrogenase (DPD)-expressing tumors who did not receive 5-fluorouracil (5-FU) when dichotomized at the mean DPD mRNA level. B: Overall survival curves for patients with low and high DPD-expressing tumors who received 5-FU.*

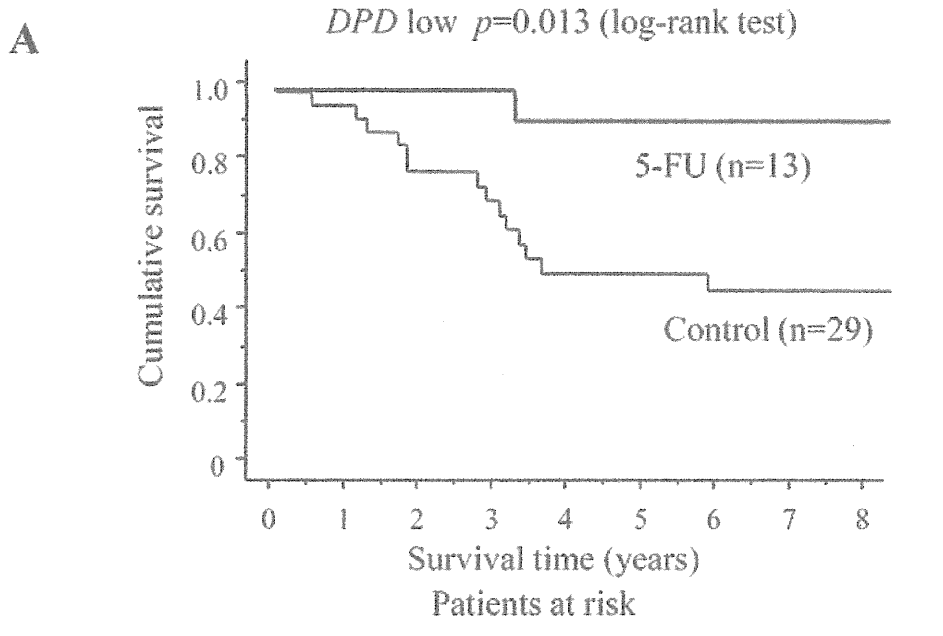

Control	29	22	13	10	5
5-FU	13	13	11	9	4

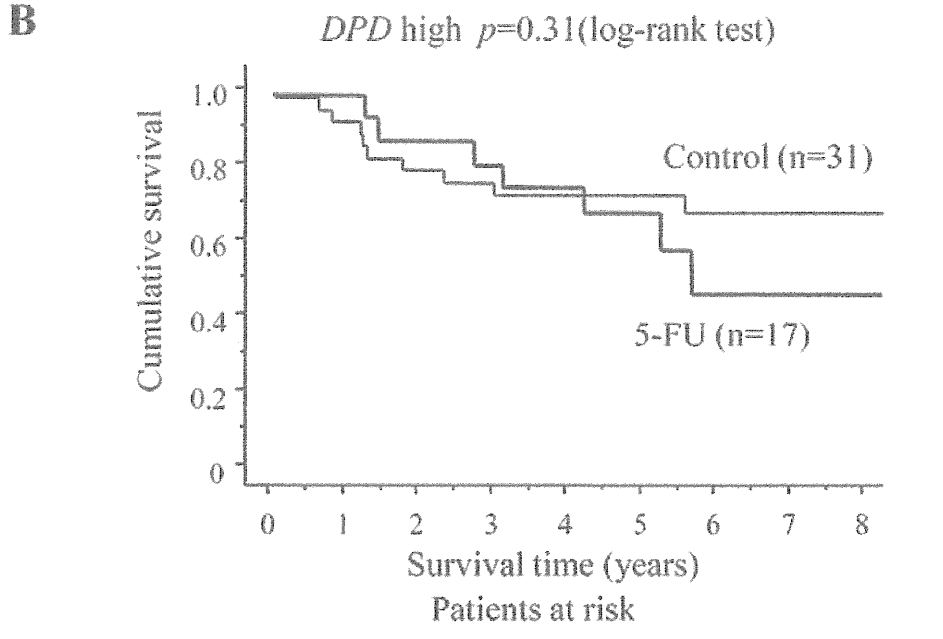

Control	31	25	19	14	7
5-FU	17	14	11	3	2

Figure 3. *A: Overall survival curves for patients with dihydropyrimidine dehydrogenase (DPD)-expressing tumors: comparison between those who underwent surgery alone and those who received 5-fluorouracil (5-FU) when dichotomized at the mean TYMS mRNA level. B: Overall survival curves for patients with high DPD-expressing tumors: comparison between those who underwent surgery alone and those who received 5-FU.*

regimens with other anticancer drugs and molecular targeting therapies for NSCLC patients with high DPD-expressing tumors are necessary.

In conclusion, using real-time RT-PCR, assessment of *TYMS* and *DPD* expressions in tumors from patients with NSCLC can provide precise prognostic information and predict the efficacy of 5-FU therapy after resection.

Conflicts of Interest Statement

The Authors have no conflicts of interest to declare.

References

1 Oguri T, Achiwa H, Bessho Y, Muramatsu H, Maeda H, Niimi T, Sato S and Ueda R: The role of thymidylate synthase and dihydropyrimidine dehydrogenase in resistance to 5-fluorouracil in human lung cancer cells. Lung Cancer *49*: 345-351,2005.

2 Kato H, Ichinose Y, Ohta M, Hata E, Tsubota N, Tada H, Watanabe Y, Wada H, Tsuboi M, Hamajima N and Ohta M; Japan Lung Cancer Research Group on Postsurgical Adjuvant Chemotherapy: A randomized trial of adjuvant chemotherapy with uracil-tegafur for adenocarcinoma of the lung. N Engl J Med *350*: 1713-1721, 2004.

3 Hamada C, Tanaka F, Ohta M, Fujimura S, Kodama K, Imaizumi M and Wada H: Meta-analysis of postoperative adjuvant chemotherapy with tegafur-uracil in non-small cell lung cancer. J Clin Oncol *23*: 4999-5006, 2005.

4 Ichinose Y, Yoshimori K, Sakai H, Nakai Y, Sugiura T, Kawahara M and Niitani H: S-1 plus cisplatin combination chemotherapy in patients with advanced non-small cell lung cancer: a multi-institutional phase II trial. Clin Cancer Res *10*: 7860-7864, 2004.

5 Danenberg PV: Thymidylate synthetase: a target enzyme in cancer chemotherapy. Biochem Biophys Acta *473*: 73-92, 1977.

6 Jonston PG, Lenz HJ and Leichman CG: Thymidylate syntase gene and protein expression correlate and are associated with response to 5-fluorouracil in human colorectal and gastric tumor. Cancer Res *55*: 1407-1412, 1995.

7 Shintani Y, Ohta M, Hirabayashi H, Tanaka H, Iuchi K, Nakagawa K, Maeda H, Kido T, Miyoshi S and Matsuda H: New prognostic indicator for non-small cell lung cancer, quantitation of thymidylate synthase by real-time reverse transcription polymerase chain reaction. Int J Cancer *104*: 790-795, 2003.

8 Fischel JL, Etienne MC, Spector T, Formento P, Renee N and Milano G: Dihydropyrimidine dehydrogenase: a tumoral target for fluorouracil modulation. Clin Cancer Res *1*: 991-6, 1995.

9 Salonga D, Danenberg KD, Johnson M, Metzger R, Groshen S, Tsao-Wei DD, Lenz HJ, Leichman CG, Leichman L, Diasio RB and Danenberg PV: Colorectal tumors responding to 5-fluorouracil have low gene expression levels of dihydropyrimidine dehydrogenase, thymidylate synthase, and thymidine phosphorylase. Clin Cancer Res *6*: 1322-1327, 2000.

10 Shintani Y, Ohta M, Hirabayashi H, Tanaka H, Iuchi K, Nakagawa K, Maeda H, Kido T, Miyoshi S and Matsuda H: Thymidylate synthase and dihydropyrimidine dehydrogenase mRNA levels in tumor tissues and the efficacy of 5-fluorouracil in patients with non-small cell lung cancer. Lung Cancer *45*: 189-196, 2004.

11 Lenz HJ, Leichman CG, and Danenberg KD: Thymidylate synthase mRNA level in adenocarcinoma of the stomach: a predictor for primary tumor response and overall survival. J Clin Oncol *14*: 176-182, 1995.

12 Yamachika T, Nakanishi H, Inada K, Tsukamoto T, Kato T, Fukushima M, Inoue M and Tatematsu M: A new prognostic factor for colorectal carcinoma, thymidylate synthase, and its therapeutic significance. Cancer *82*: 70-77, 1998.

13 Harris BE, Song R, Soong SJ and Diasio RB: Relationship between dihydropyrimidine dehydrogenase activity and plasma 5-fluorouracil levels with evidence for circadian variation of enzyme activity and plasma drug levels in cancer patients receiving 5-fluorouracil by protracted continuous infusion. Cancer Res *50*: 197-201, 1990.

14 Nakano J, Huang C, Liu D, Masuya D, Nakashima T, Yokomise H, Ueno M, Wada H and Fukushima M: Evaluations of biomarkers associated with 5-FU sensitivity for non-small cell lung cancer patients postoperatively treated with UFT. Br J Cancer *95*: 607-615, 2006.

15 Takizawa M, Kawakami K, Obata T, Matsumoto I, Ohta Y, Oda M, Sasaki T and Watanabe G: *In vitro* sensitivity to platinum-derived drugs is associated with expression of thymidylate synthase and dihydropyrimidine dehydrogenase in human lung cancer. Oncol Rep 15: 1533-1539, 2006.

16 Takeda M, Okamoto I, Hirabayashi N, Kitano M and Nakagawa K: Thymidylate synthase and dihydropyrimidine dehydrogenase expression levels are associated with response to S-1 plus carboplatin in advanced non-small cell lung cancer. Lung Cancer *73*: 103-109, 2011.

Received September 13, 2011
Revised November 17, 2011
Accepted November 18, 2011

Oncogene (2011) 30, 3489–3501

www.nature.com/onc

ORIGINAL ARTICLE

MicroRNA-mediated downregulation of mTOR/FGFR3 controls tumor growth induced by Src-related oncogenic pathways

C Oneyama[1], J Ikeda[2], D Okuzaki[3], K Suzuki[1], T Kanou[1,4], Y Shintani[4], E Morii[2], M Okumura[4], K Aozasa[2] and M Okada[1]

[1]Department of Oncogene Research, Research Institute for Microbial Diseases, Osaka University, Suita, Osaka, Japan; [2]Department of Pathology, Graduate School of Medicine, Osaka University, Suita, Osaka, Japan; [3]DNA-chip Developmental Center for Infectious Diseases, Research Institute for Microbial Diseases, Osaka University, Suita, Osaka, Japan and [4]Department of General Thoracic Surgery, Graduate School of Medicine, Osaka University, Suita, Osaka, Japan

The tyrosine kinase c-Src is upregulated in various human cancers, but the molecular mechanisms underlying c-Src-mediated tumor growth remain unclear. Here we examined the involvement of microRNAs in the c-Src-mediated tumor growth. Microarray profiling revealed that c-Src activation downregulates a limited set of microRNAs, including miR-99a, which targets oncogenic mammalian target of rapamycin (mTOR) and fibroblast growth factor receptor 3 (FGFR3). Re-expression of miR-99a suppressed tumor growth of c-Src-transformed cells, and this effect was restored by the overexpression of mTOR. The downregulation of miR-99a was also observed in epidermal growth factor- and Ras-transformed cells, and it was suppressed by inhibiting the mitogen-activated protein kinase (MAPK) pathway. Furthermore, miR-99a downregulation is associated with mTOR/FGFR3 upregulation in various human lung cancer cells/tissues. The tumorigenicity of these cells was suppressed by the introduction of miR-99a. These findings suggest that the miR-99a-mTOR/FGFR3 pathway is crucial for controlling tumor growth in a wide range of human cancers that harbor upregulation of the Src-related oncogenic pathways.
Oncogene (2011) **30**, 3489–3501; doi:10.1038/onc.2011.63; published online 7 March 2011

Keywords: c-Src; tumor; miRNA; mTOR; FGFR3

Introduction

The tyrosine kinase c-Src is a pivotal component of multiple signaling pathways that regulate cell proliferation, survival, adhesion and migration, which are processes tightly associated with tumor progression (Brown and Cooper, 1996; Ingley, 2008). c-Src is frequently overexpressed and activated in a wide variety of human cancers, suggesting a role in tumor progression (Frame, 2002; Ishizawar and Parsons, 2004; Yeatman, 2004). In normal cells, the kinase activity of c-Src is rigorously controlled by the C-terminal Src kinase (Csk) (Nada *et al.*, 1991; Okada *et al.*, 1991); therefore, the oncogenic potential of c-Src is suppressed even when c-Src is abundantly expressed. In some cancer cells, however, c-Src function is upregulated despite the fact that the *c-src* gene is rarely mutated (Irby *et al.*, 1999; Irby and Yeatman, 2000). Thus, it is considered that disruption of the strict regulation of c-Src may trigger cancer progression, although the underlying mechanisms remain unclear. Once activated, c-Src acts as a common upstream regulator of various oncogenic pathways, including the Ras/MAPK pathway, STAT and phosphoinositide 3-kinase (PI3K) pathways (Ingley, 2008), to induce the phenotypic changes characteristic of cell transformation. Mounting evidence shows the importance of c-Src in cancer progression, but the complexity of c-Src function has hampered the elucidation of the critical c-Src pathways involved in directing tumor growth.

MicroRNAs (miRNAs) are a class of small RNA molecules approximately 22 nucleotides long that regulate gene expression by blocking mRNA translation and/or mediating mRNA degradation (Ambros, 2004; Bartel, 2004, 2009; Ventura and Jacks, 2009). More than 600 different miRNAs have so far been identified in human beings, and they have been shown to control diverse cellular functions, including cell proliferation and differentiation (He and Hannon, 2004; Bartel, 2009). Each miRNA is predicted to target hundreds of genes, and each transcript may interact with multiple miRNAs (Bartel, 2009). This interplay between miRNA and transcripts underscores the potential role of miRNAs as key regulators of complex signaling networks. In recent years, numerous studies have shown aberrant expression of miRNAs in human cancers (Calin and Croce, 2006; Esquela-Kerscher and Slack, 2006). In addition, some miRNAs are located in unstable genomic regions and are often downregulated in tumors (Calin and Croce, 2006). These lines of evidence strongly suggest that a group of miRNAs functions as oncogenes or tumor suppressors (Shenouda and Alahari, 2009).

Correspondence: Dr C Oneyama, Department of Oncogene Research, Research Institute for Microbial Diseases, Osaka University, 3-1 Yamadaoka, Suita, Osaka 565-0871, Japan.
E-mail: coneyama@biken.osaka-u.ac.jp
Received 3 November 2010; revised 16 January 2011; accepted 4 February 2011; published online 7 March 2011

The PI3K pathway is a key signal-transduction system that links multiple receptors and oncogenic molecules to diverse cellular functions and is inappropriately activated in many human cancers (Engelman, 2009; Liu *et al.*, 2009). Mammalian target of rapamycin (mTOR) is a serine–threonine kinase that is a major downstream effector of the PI3K pathway and plays a crucial part in the regulation of cell growth by monitoring nutrient availability, cellular energy levels, oxygen levels and mitogenic signals (Wullschleger *et al.*, 2006). The mTOR signaling pathway has also been implicated in tumorigenesis (Petroulakis *et al.*, 2006; Guertin and Sabatini, 2007; Nagaraja *et al.*, 2010). Indeed, rapamycin, a selective mTORC1 inhibitor, has antineoplastic properties, and its analogues have been developed as anticancer drugs. Major downstream targets of mTORC1 are ribosomal protein S6 kinase 1 (S6K1, also known as p70S6K) and eukaryotic translation initiation factor 4E-binding protein 1, both of which play crucial roles in the regulation of protein synthesis (Hay and Sonenberg, 2004). Therefore, activation of the mTOR pathway provides tumor cells with a growth advantage by promoting protein synthesis (Sabatini, 2006; Menon and Manning, 2008). In human cancers, the PI3K pathway is activated by either upregulation of receptor tyrosine kinases or somatic mutations in specific components of the pathway (Liu *et al.*, 2009). Fibroblast growth factor receptor 3 (FGFR3) is one of the receptors that promote cell survival by stimulating PI3K-AKT signaling (Ong *et al.*, 2001). Overexpression and/or mutation of FGFR3 are frequently observed in myeloma, ovarian and bladder cancers, suggesting that this molecule plays a role in tumorigenesis (van Rhijn *et al.*, 2001; Eswarakumar *et al.*, 2005).

To address the molecular mechanisms underlying c-Src-mediated cell transformation, we previously developed a model system using Csk-deficient fibroblasts ($Csk^{-/-}$ cells) that can be transformed by wild-type c-Src (Oneyama *et al.*, 2008). In this system, the activation of relatively small numbers of molecules is sufficient for induction of cell transformation and tumorigenesis (Oneyama *et al.*, 2008). These findings suggest that this system could be useful in the identification of critical pathways leading to c-Src transformation. In this study, this experimental system was applied for the analysis of potential contribution of miRNAs to c-Src-mediated tumor growth. Expression profiling of miRNAs in $Csk^{-/-}$ cells revealed that a limited set of miRNAs are differentially regulated by c-Src transformation. In particular, we focused our analysis on miR-99a based on its significant downregulation by c-Src transformation. We show that miR-99a is downregulated in various human cancers and targets *mTOR* and *FGFR3* genes that are tightly associated with human cancers. Functional analysis of miR-99a in c-Src/Ras-transformed cells and various human cancer cells/tissues suggests that miR-99a is downregulated by the activation of Src-related oncogenic pathways and functions as a suppressor of tumor growth by controlling the expression of mTOR/FGFR3.

Results

miRNA expression profiling in c-Src-transformed cells

Previously, we developed an experimental system using $Csk^{-/-}$ cells to analyze the molecular mechanisms underlying c-Src-mediated transformation (Oneyama *et al.*, 2008). Despite the activation of endogenous c-Src, the cells do not transform owing to the substantial degradation of activated c-Src by the ubiquitin–proteasome system (Hakak and Martin, 1999). However, exogenous expression of c-Src, at levels over twice the endogenous level, efficiently induced cell transformation (Oneyama *et al.*, 2008). Using these cells, we compared the expression profiles of miRNAs between non-transformed cells ($Csk^{-/-}$ cells and those expressing Csk or c-Src plus Csk) and c-Src-transformed cells ($Csk^{-/-}$ cells expressing c-Src) through miRNA microarray analysis. Pair-wise significance analysis of the microarray data (see Supplementary information) indicated that seven *miRNA* genes were downregulated (Figure 1a) and six *miRNA* genes were significantly upregulated in c-Src-transformed cells.

Quantitative real-time PCR (qRT–PCR) analyses confirmed the downregulation of the seven miRNAs in c-Src-transformed cells (Figure 1b). These miRNAs were categorized into three clusters based on their chromosomal locations of mouse: miR-23b and -27b are located on chromosome (Chr.) 13, miR-322, -450a, -503 and -542 are on Chr. X, and miR-99a is on Chr. 16. These findings suggest a potential role of these miRNAs in regulating transformation via the c-Src-mediated pathway.

miR-99a as a suppressor of c-Src-induced tumor growth

Recent studies have reported that miR-99a is transcribed from the commonly deleted region at 21q21 in human lung cancers (Nagayama *et al.*, 2007; Yamada *et al.*, 2008) and that miR-99a is downregulated in ovarian carcinoma (Nam *et al.*, 2008), squamous cell carcinoma of the tongue (Wong *et al.*, 2008), bladder cancer (Catto *et al.*, 2009), squamous cell lung carcinoma (Gao *et al.*, 2010) and childhood adrenocortical tumors (Doghman *et al.*, 2010). These findings indicate that miR-99a is widely downregulated in human cancers, suggesting a potential role for miR-99a as a tumor suppressor. Thus, we further concentrated on miR-99a and tested if miR-99a is involved in regulating c-Src-induced transformation and tumor growth. Overexpression of miR-99a did not induce changes in cell morphology or cytoskeletal organization of c-Src-transformed cells (Figure 2a). In addition, miR-99a expression did not affect c-Src-induced tyrosine phosphorylation of cellular proteins or the activity of c-Src (pY416) or Erk (p-Erk), although it slightly inhibited AKT activity (Figure 2b). An *in vitro* proliferation assay showed that miR-99a expression only weakly suppressed anchorage-dependent growth of these cells (Supplementary Figure 1). However, a colony formation assay in soft agar revealed that miR-99a expression dramatically suppressed anchorage-independent growth of c-Src-transformed cells in a dose-dependent manner

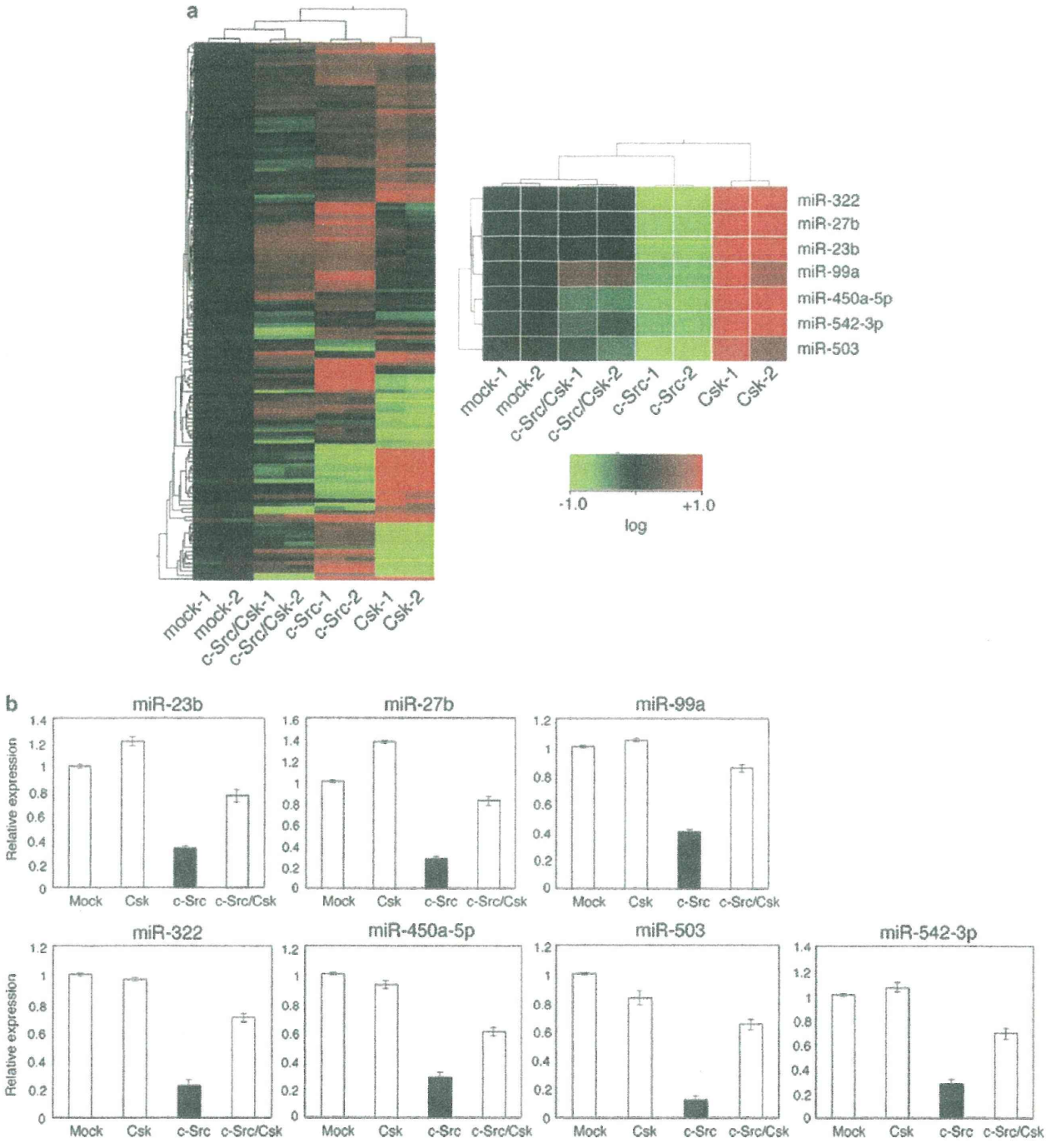

Figure 1 miRNA expression profiling in c-Src-transformed cells. (**a**) Hierarchical clustering of 138 miRNAs that exhibited significantly altered expression in c-Src/Csk-, c-Src- or Csk-expressing cells compared with mock $Csk^{-/-}$ cells is shown as described in the Supplementary information (left side). Of the 138 miRNAs, seven miRNAs (miR-322, -27b, -23b, -99a, -450a-5p, -542-3p and -503) that downregulated twofold in c-Src-transformed cells were subjected to hierarchical clustering (right side). In each panel, the selected miRNAs are shown in the lines and four pairs of duplicates in the columns. The color bar indicates the fold-change (log 2). Red denotes upregulated and green denotes downregulated. (**b**) The expression of seven miRNAs downregulated was analyzed using qRT–PCR. Relative values ± s.d. were obtained from three independent assays.

(Figure 2c). Tumorigenesis of c-Src-transformed cells in nude mice was also remarkably suppressed by the expression of miR-99a (Figure 2d). These results suggest that miR-99a functions as a suppressor of tumor growth induced by the activation of c-Src in these cells.

miR-99a targets mTOR and FGFR3

To elucidate the function of miR-99a, we performed a bioinformatic search (Targetscan and Pictar) for putative targets of miR-99a. Interestingly, miR-99a was found to have relatively few potential targets

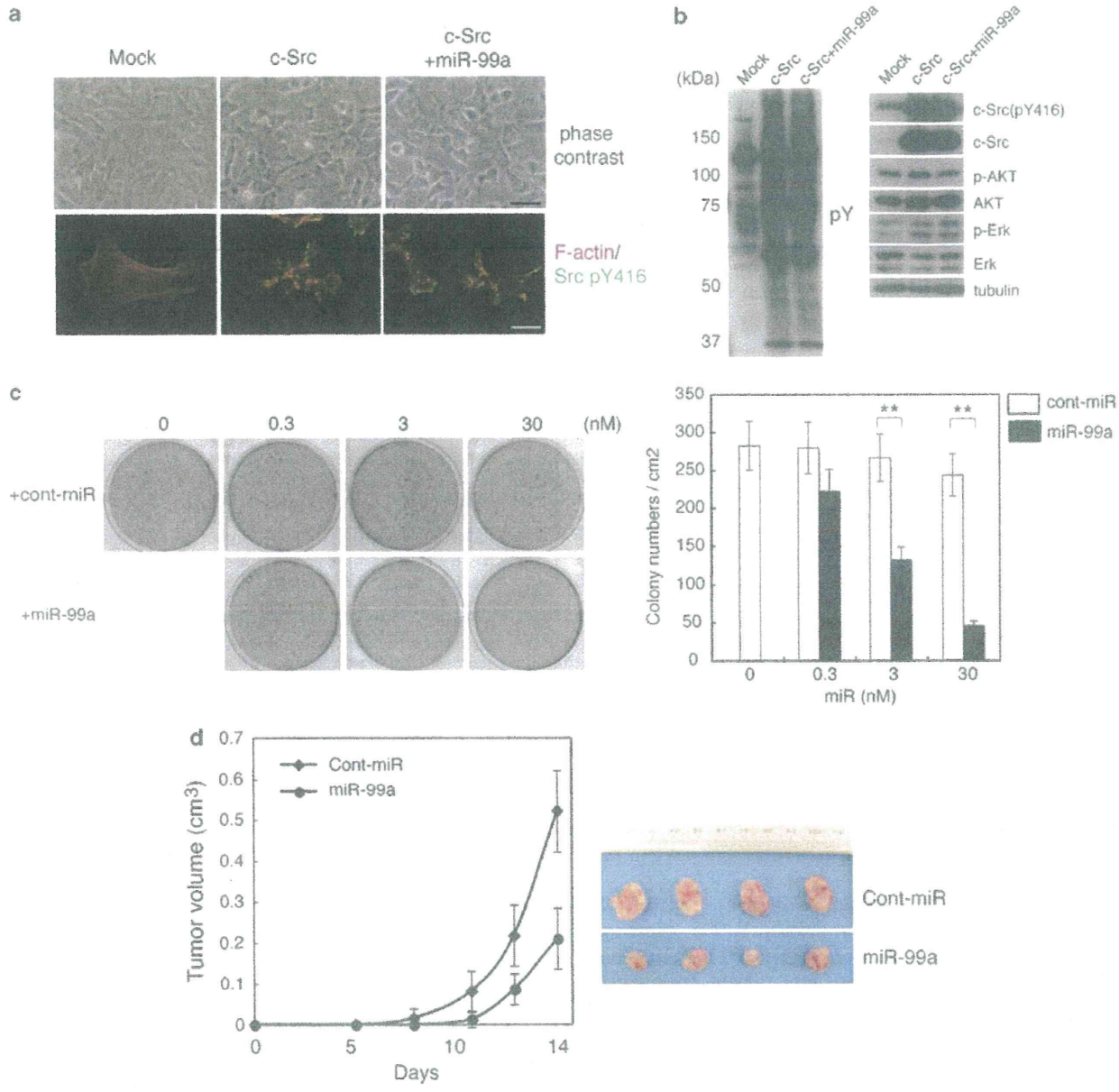

Figure 2 miR-99a as a suppresser of c-Src-induced tumor growth. (**a**) The morphology of $Csk^{-/-}$ cells expressing c-Src and miR-99a was observed under phase-contrast microscopy (upper panels). Actin filaments (red) and intracellular localization of activated Src (Src pY416: green) in the indicated cells were analyzed by immunostaining (lower panels). A white and a black scale bar represents 20 and 50 μm, respectively. (**b**) Total cell lysates from $Csk^{-/-}$ cells expressing c-Src and miR-99a were immunoblotted with the antibodies indicated. (**c**) Soft-agar colony formation assays of c-Src-transformed cells treated with 0.3–30 nM of miR-99a or control (cont-miR). Representative dishes from three independent experiments are shown (left panels). The mean number of colonies ± s.d. was obtained from three independent experiments (right panel). (**d**) The effect of miR-99a expression on tumorigenicity in nude mice. c-Src-transformed cells treated with miR-99a were inoculated subcutaneously into nude mice. Averages ± s.d. of tumor volume (cm^3) obtained from four mice are plotted vs time after inoculation (days). Excised tumors are shown in the right panels.

(around 40), which included several cell signaling molecules. Among the candidates, the 3′-untranslated regions of mTOR and FGFR3 contained regions that matched the seed sequences of miR-99a (Figure 3a). A luciferase reporter assay in c-Src-transformed cells showed that miR-99a specifically targeted the miR-99a binding sequences in mTOR and FGFR3 mRNAs (Figure 3b). Conversely, introduction of anti-miR-99a enhanced the expression of luciferase reporter of both constructs in non-transformed $Csk^{-/-}$ cells, which express miR-99a at higher levels (Figure 3c). These results indicate that miR-99a can directly target mTOR and FGFR3 mRNA to regulate their expression.

We then examined the impact of miR-99a expression on the endogenous mTOR and FGFR3 proteins. Western blot analysis showed that both proteins were upregulated by c-Src transformation (Figure 3d, lanes 1 vs 3), whereas they were significantly downregulated by

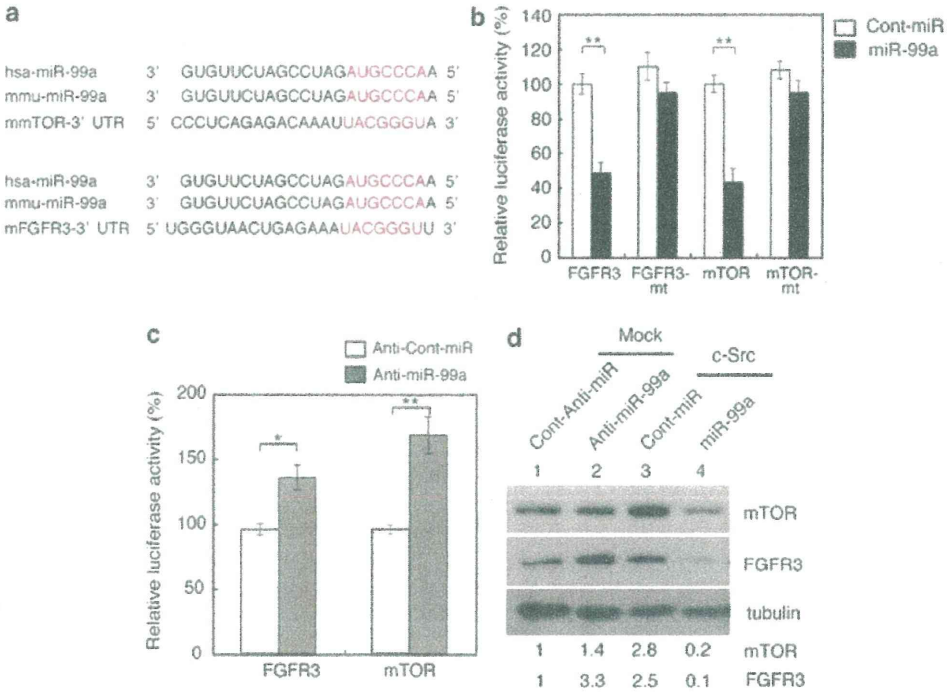

Figure 3 miR-99a targets mTOR and FGFR3. (**a**) Alignment of RNA sequences of human and mouse miR-99a and the potential miR-99a binding sequences in the mTOR and FGFR3 3′-untranslated regions. The seed sequence of miR-99a and its binding sequences are shown in red. (**b**) pMIR-mTOR and pMIR-FGFR3 luciferase reporter constructs, containing either wild-type or mutated (mt) mTOR and FGFR3 3′-untranslated regions, were transfected into c-Src-transformed cells. Relative *Renilla* luciferase expression was standardized to a transfection control. Relative values ± s.d. were obtained from three independent assays. (**c**) $Csk^{-/-}$ cells treated with anti-cont-miR or anti-miR-99a were transfected with pMIR-mTOR and pMIR-FGFR3 constructs, and the relative luciferase activity was determined. Relative values ± s.d. were obtained from three independent assays. (**d**) $Csk^{-/-}$ cells (Mock) were transfected with the control or anti-miR-99a, and c-Src-transformed cells (c-Src) were transfected with the control or miR-99a. Total cell lysates were immunoblotted with the indicated antibodies. The relative expression levels of mTOR or FGFR3 are shown at the bottom of the panels. $*P<0.05$ and $**P<0.01$, by Student's *t*-test.

the expression of miR-99a (lanes 3 vs 4). In contrast, inactivation of miR-99a by anti-miR-99a increased mTOR and FGFR3 expressions (lanes 1 vs 2). These findings show that miR-99a can target endogenous mTOR/FGFR3, and suggest that downregulation of miR-99a by c-Src activation is tightly associated with the upregulation of mTOR/FGFR3 in c-Src-transformed cells.

Roles of mTOR and FGFR3 in c-Src-mediated tumor growth

To examine the role of upregulation of mTOR and FGFR3 in c-Src-transformed cells, we performed rescue experiments using open-reading frames (ORFs) of mTOR and FGFR3 cDNAs. The expression of miR-99a in c-Src-transformed cells reduced mTOR protein levels as well as the activity of p70S6K, a critical downstream effector of mTOR (Figure 4a, lane 2). When the mTOR ORF was introduced into miR-99a-treated cells, mTOR protein and the activity of p70S6K were significantly increased (Figure 4a, lane 4). Although the extent of these upregulations was not so remarkable, it was sufficient to restore a significant colony-forming activity in these cells (Figure 4b). We also observed that inhibition of mTOR activity with the selective inhibitor rapamycin effectively suppressed tumor growth of c-Src-transformed cells as well as A549 cells that have c-Src upregulation (Supplementary Figure 2). These findings suggest that the mTOR activity is correlated with the ability of c-Src to induce tumor growth.

To further verify the significance of upregulation of mTOR protein levels in tumor growth, we differentially overexpressed mTOR protein in non-transformed $Csk^{-/-}$ cells, in which c-Src is activated insufficiently for cell transformation (Oneyama *et al.*, 2008). The expression of mTOR protein dose-dependently enhanced p70S6K activity and the colony-forming activity of these cells, and the expression of mTOR at nearly twice the normal level was sufficient to induce colony formation (Figure 4c). More interestingly, when mTOR was upregulated by inactivating miR-99a using anti-miR-99a, non-transformed $Csk^{-/-}$ cells gained the ability to form colonies in a manner dependent on the concentrations of anti-miR-99a (Figure 4d and Supplementary Figure 3). These results suggest that mTOR can dose-dependently control the potential for tumor growth, within a range regulatable by miR-99a. However, the colony-forming activity of mTOR-overexpressing cells (Figure 4c, lane 3) was significantly weaker than that of c-Src-transformed cells (Figure 4c, lane 4

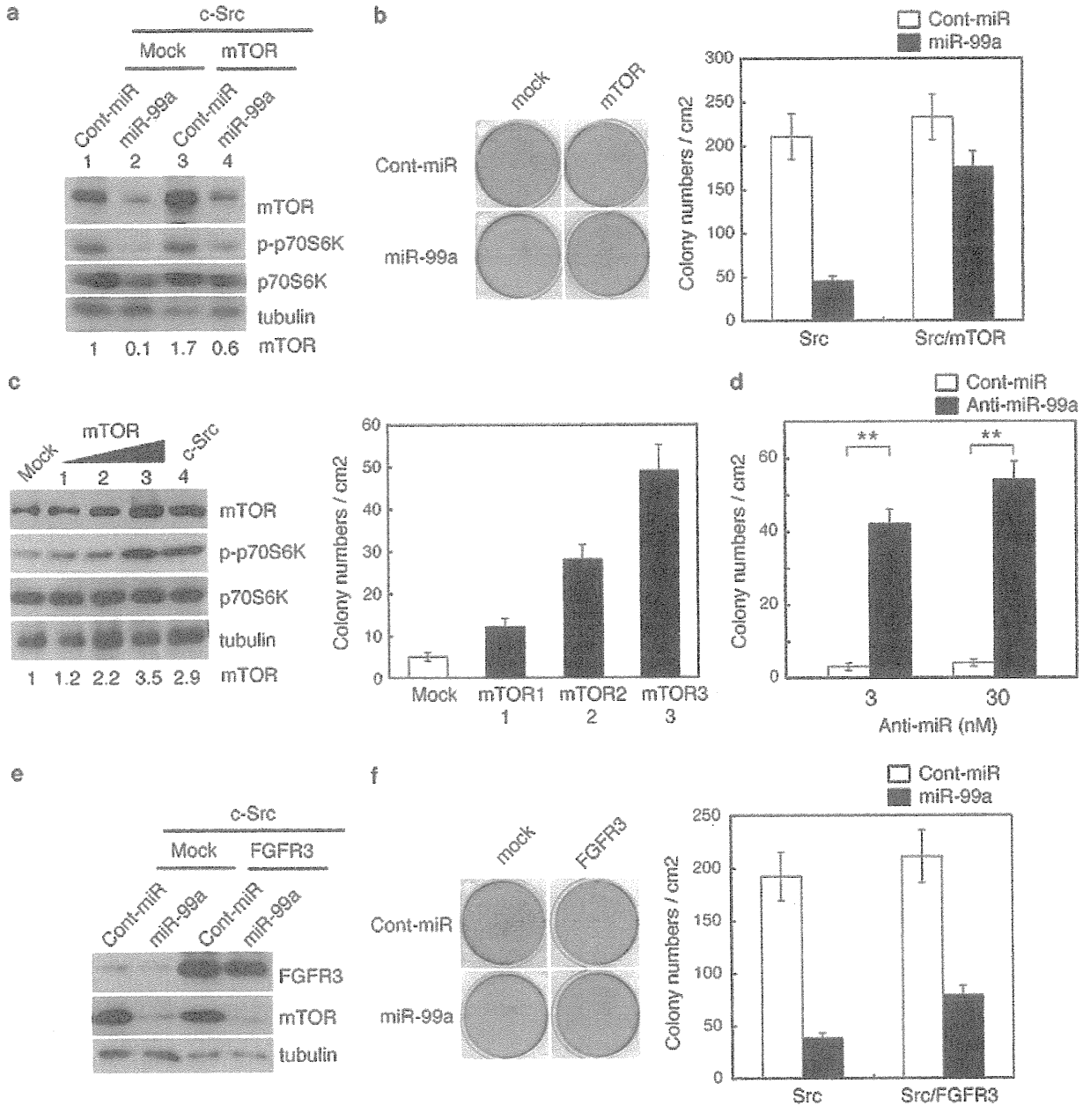

Figure 4 Roles of mTOR and FGFR3 in c-Src-mediated tumor growth. (**a**) c-Src-transformed cells transfected with the mTOR ORF cDNA were treated with cont-miR or miR-99a, and the total cell lysates were immunoblotted with the indicated antibodies. The relative expression levels of mTOR are shown at the bottom of the panels. (**b**) Soft-agar colony formation assays for cells used in (**a**). Representative dishes from three independent experiments are shown (left panels). The mean number of colonies ± s.d. was obtained from three independent experiments (right panel). (**c**) Total cell lysates of Csk $^{-/-}$ cells expressing different amounts of mTOR were immunoblotted with the indicated antibodies (left panels). The relative expression levels of mTOR are shown at the bottom of the panels. The cells were subjected to soft-agar colony formation assays (right panel). The mean number of colonies ± s.d. was obtained from three independent experiments (right panel). (**d**) Soft-agar colony formation assays of Csk$^{-/-}$ cells treated with indicated concentrations of anti-miR-99a or anti-cont-miR. The mean number of colonies ± s.d. was obtained from three independent experiments. $^{**}P<0.01$, by Student's *t*-test. (**e**) c-Src-transformed cells transfected with the FGFR3 ORF cDNA were treated with cont-miR or miR-99a, and the total cell lysates were immunoblotted with the indicated antibodies. (**f**) Soft-agar colony formation assays for cells used in (**e**). The mean number of colonies ± s.d. was obtained from three independent experiments (right panel).

and Figure 2c). This indicates that mTOR is required, but insufficient for inducing full transformation, because critical pathways, such as the MAPK pathway, which are required for cell proliferation, were not activated by the expression of mTOR.

On the other hand, the transfection of c-Src-transformed cells with the FGFR3 ORF induced a substantial overexpression of FGFR3 protein even in miR-99a-treated cells (Figure 4e), but it only moderately rescued c-Src-mediated tumor growth (Figure 4f).

However, it should be noted that mTOR was also downregulated by miR-99a even in FGFR3-overexpressing cells. Thus, it seems probable that the recovery of tumor growth by FGFR3 expression may be cancelled by the downregulation of mTOR. In contrast, the selective FGFR3 inhibitor PD173074 (Trudel *et al.*, 2004) was able to dose-dependently suppress colony-forming activity of c-Src-transformed cells and A549 cells (Supplementary Figure 4). Therefore, it is likely that upregulation of FGFR3 can also contribute to c-Src-mediated tumor growth by acting upstream of mTOR.

miR-99a is downregulated by Src-related oncogenic pathways

To follow the signaling pathway leading to the downregulation of miR-99a, we first tested the contribution of epidermal growth factor receptor (EGFR) signaling involving c-Src activation. When murine embryonic fibroblasts (MEFs) were stimulated with EGF, the kinase activity of c-Src was increased by auto-phosphorylation at Y418 (Figure 5a, left panels), and the cells showed morphological transformation (data not shown). In these EGF-transformed cells, the expression of miR-99a was appreciably downregulated (Figure 5b). Conversely, the expression of mTOR and FGFR3 was upregulated by EGF stimulation (Figure 5a, right panels). These results indicate that the expression of miR-99a can also be regulated downstream of EGFR signaling. To further identify the pathway downstream of this EGFR signaling, we examined the effect of an MAPK/ERK kinase (MEK) inhibitor (U0126) or a PI3K inhibitor (LY294002) on EGF-induced downregulation of miR-99a. The expression of miR-99a was significantly restored by treatment with U0126, but not by LY294002 (Figure 5c), suggesting that miR-99a expression is mainly regulated via the MEK/ERK pathway.

These findings led to the question as to whether the downregulation of miR-99a can be induced by other oncogenes such as v-Src, H-RasV12 and K-RasG12, all of which can activate the MEK/ERK pathway. As expected, transformation by these oncogenes induced a significant downregulation of miR-99a to a level similar to that observed in c-Src-transformed cells (Figures 5d and 1b), and inversely caused upregulation of mTOR and FGFR3 proteins (Figure 5e). The ectopic expression of miR-99a in these cells downregulated mTOR and FGFR3 proteins (Figure 5e) and significantly suppressed their colony-forming activities (Figure 5f). These findings suggest that the expression of miR-99a can be downregulated via the Ras-MEK/ERK pathway downstream of activated EGFR/Src.

miR-99a in human cancer cells

To examine if the miR-99a–mTOR/FGFR3 axis is indeed functional in human cancers, we determined the expression levels of miR-99a and mTOR/FGFR3 in several human lung cancer cell lines. Western blot analysis showed a significant upregulation of mTOR and FGFR3 in all of the lung cancer cell lines examined (Figure 6a). In contrast, qRT–PCR analysis revealed that the expression of miR-99a was greatly reduced in most of the lung cancer cells (Figure 6b). The levels of mTOR and FGFR3 were not necessarily correlated with the amount of protein or the activity status of c-Src (pY418), which reflects the potential contribution of other signaling components to human cancers (Figure 6a). Human cancer cells contain multiple mutations in oncogenes and tumor suppressor genes. A549 has c-Src upregulation and a *K-Ras* mutation; Lu99 harbors a *K-Ras* mutation; H69 and H526 have an *N-myc* amplification; PC9 has an *EGFR* mutation; and PC10 has a c-Src upregulation as well as a *PTEN* mutation (Yokota and Kohno, 2004; Noro *et al.*, 2006). These lines of information suggest that there is an upregulation of the Src-related oncogenic pathways in these cells, which may account for the downregulation of miR-99a observed in various human cancer cells.

To examine the functional link between miR-99a and mTOR/FGFR3 in human cancers, we ectopically expressed miR-99a in lung (A549, PC10 and Lu99) cancer cells. The expression of miR-99a in A549 cells induced a significant downregulation of mTOR and FGFR3 proteins (Figure 6c) and significantly suppressed the colony-forming activity of A549, PC10 and Lu99 cells (Figure 6d). Conversely, knockdown of miR-99a in A549 cells increased mTOR and FGFR3 expressions and colony-forming activity (Figures 6c and e). In addition, inactivation of miR-99a induced an anchorage-independent growth in human normal epithelial cells such as HEK293 and HaCaT (Supplementary Figure S5). These results suggest that miR-99a downregulation is involved in carcinogenesis and malignancy in human cells.

The importance of mTOR upregulation in tumor growth was further confirmed by observing that short hairpin RNA-mediated mTOR knockdown in A549 cells appreciably suppressed colony-forming activity (Supplementary Figure S6). Interestingly, the effect of miR-99a expression was more evident *in vivo*: tumorigenesis in nude mice was potently suppressed by miR-99a expression in A549 cells (Figure 6f). These findings suggest that miR-99a is involved in regulating tumor growth of a subset of human cancer cells by targeting mTOR/FGFR3.

miR-99a in human cancer tissues

Finally, we verified the role of miR-99a in human cancers by determining miR-99a expression in lung primary tumors as well as in adjacent normal tissues using qRT–PCR. In most of the tumor samples examined, miR-99a was significantly downregulated (Figure 7a). Immunohistochemical analysis of mTOR and FGFR3 expression in lung tumor specimens showed that mTOR and FGFR3 immunoreactivity was greatly increased in all of the five primary tumor regions in comparison to the adjacent normal tissues (Figure 7b). These observations suggest that there is an inverse correlation between the expressions of miR-99a and mTOR/FGFR3 even in human cancer tissues.

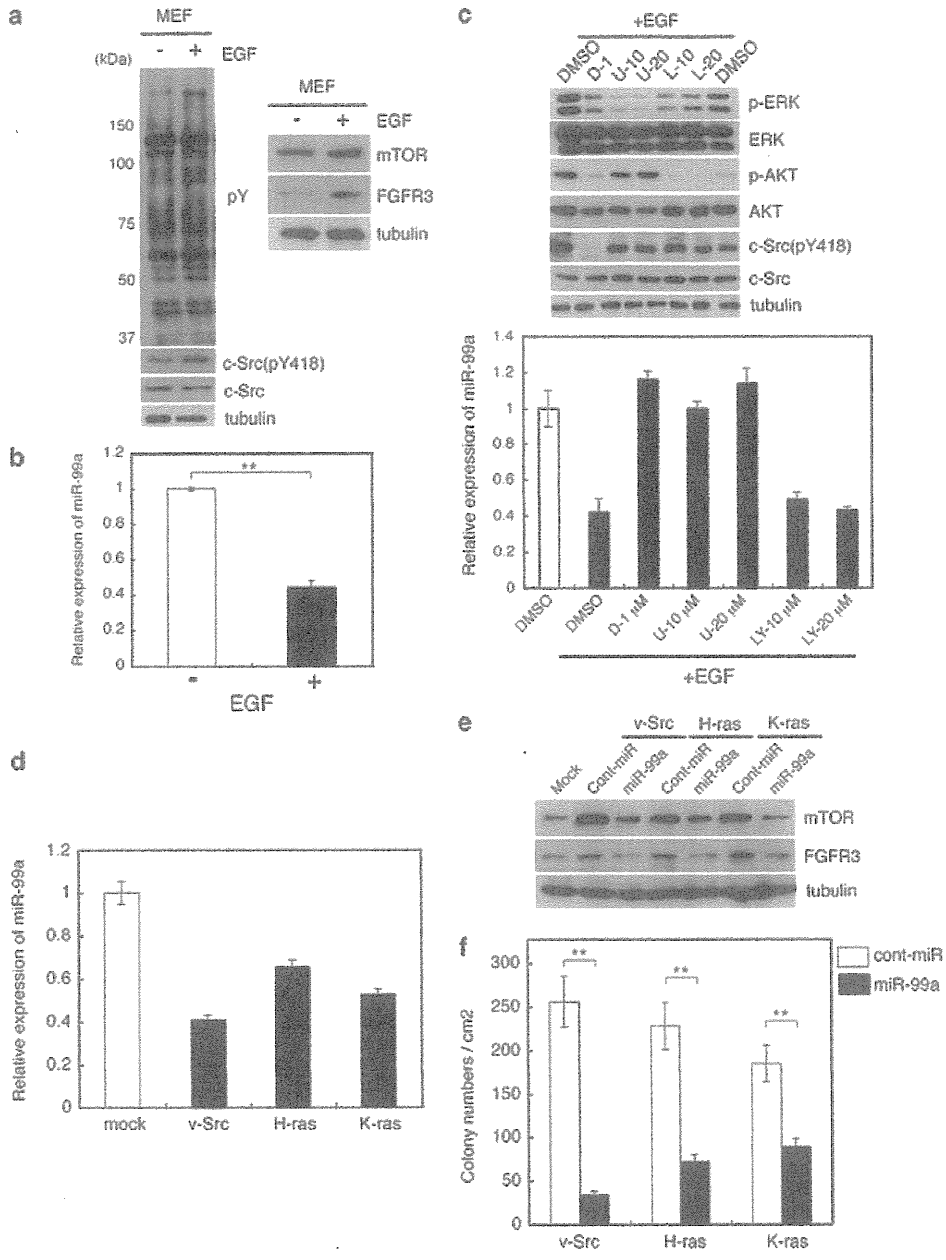

Figure 5 miR-99a is downregulated in cells transformed by other oncogenic signals. (**a**) Total cell lysates from MEFs were stimulated with or without 10 ng/ml EGF for 4 days and immunoblotted with the antibodies indicated. (**b**) miR-99a expression levels were assessed by qRT–PCR in MEFs stimulated with (black) or without (white) EGF. (**c**) MEFs were treated with or without Dasatinib (D), U0126 (U) or LY294002 (L) at the indicated concentrations in the presence of EGF for 2 days, and the total cell lysates were immunoblotted with the antibodies indicated (upper panels). The expression levels of miR-99a were assessed by qRT–PCR (lower panel). (**d**) The expression levels of miR-99a in MEFs transformed by v-Src, H-RasV12 or K-RasG12 were assessed by qRT–PCR. Relative values ± s.d. were obtained from three independent assays (**b–d**). (**e**) MEFs transformed by v-Src, H-RasV12 or K-RasG12 were treated with cont-miR or miR-99a, and the total cell lysates were immunoblotted with the antibodies indicated. (**f**) MEFs analyzed in (**e**) were subjected to soft-agar colony formation assay. The mean number of colonies ± s.d. was obtained from three independent experiments. $^{**}P<0.01$, by Student's *t*-test.

Overall, the present findings suggest that downregulation of miR-99a is induced by the activation of Src-related oncogenic pathways in various human cancers, and is tightly associated with the promotion of tumor growth via upregulation of mTOR/FGFR3 pathways (Figure 7c).

Discussion

To elucidate the molecular mechanisms underlying c-Src-mediated transformation, we previously established an experimental system using Csk-deficient cells (Oneyama *et al*., 2008). In this study, we used this

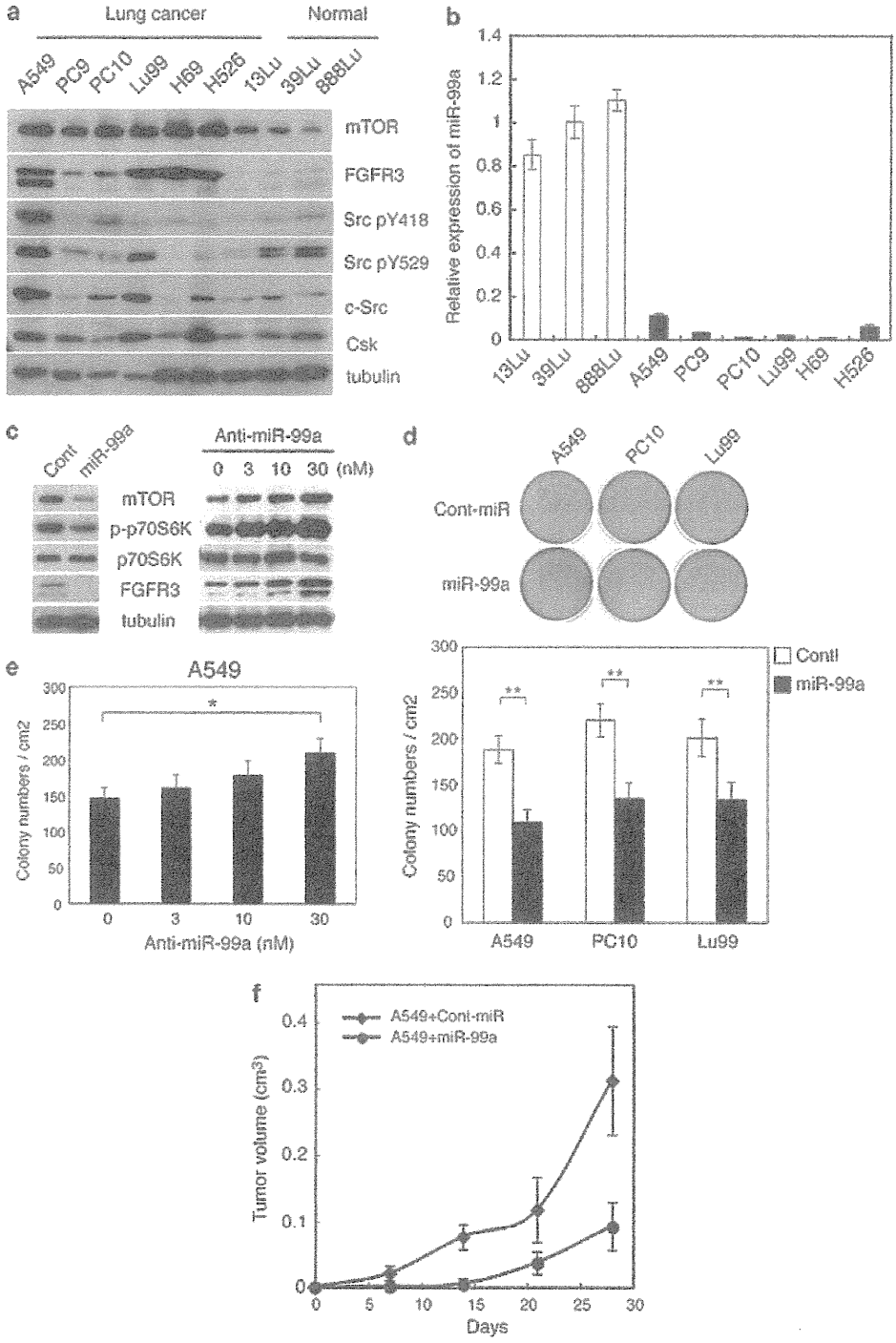

Figure 6 miR-99a in human lung cancer cells. (**a**) Total cell lysates from the indicated lung cancer cell lines were immunoblotted with the indicated antibodies. (**b**) The expression levels of miR-99a in these cells were assessed by qRT–PCR. The mean values ± s.d. were obtained from three independent experiments. (**c**) A549 cells were transfected with miR-99a or anti-miR-99a, followed by immunoblotting with the indicated antibodies. (**d**) A549, PC10 and Lu99 cells were treated with miR-99a or control-miR were subjected to the soft-agar colony formation assay. Representative dishes from three independent experiments are shown (upper panels). The mean number of colonies ± s.d. was obtained from three independent experiments in each case (lower panel). (e) Soft-agar colony formation assays of A549 cells treated with indicated concentrations of anti-miR-99a. The mean number of colonies ± s.d. was obtained from three independent experiments. (**f**) A549 cells transfected with or without miR-99a were inoculated subcutaneously into nude mice. Means ± s.d. of tumor volume (cm^3) obtained from three mice are plotted vs time after inoculation (days). $^*P<0.05$ and $^{**}P<0.01$, by Student's *t*-test.

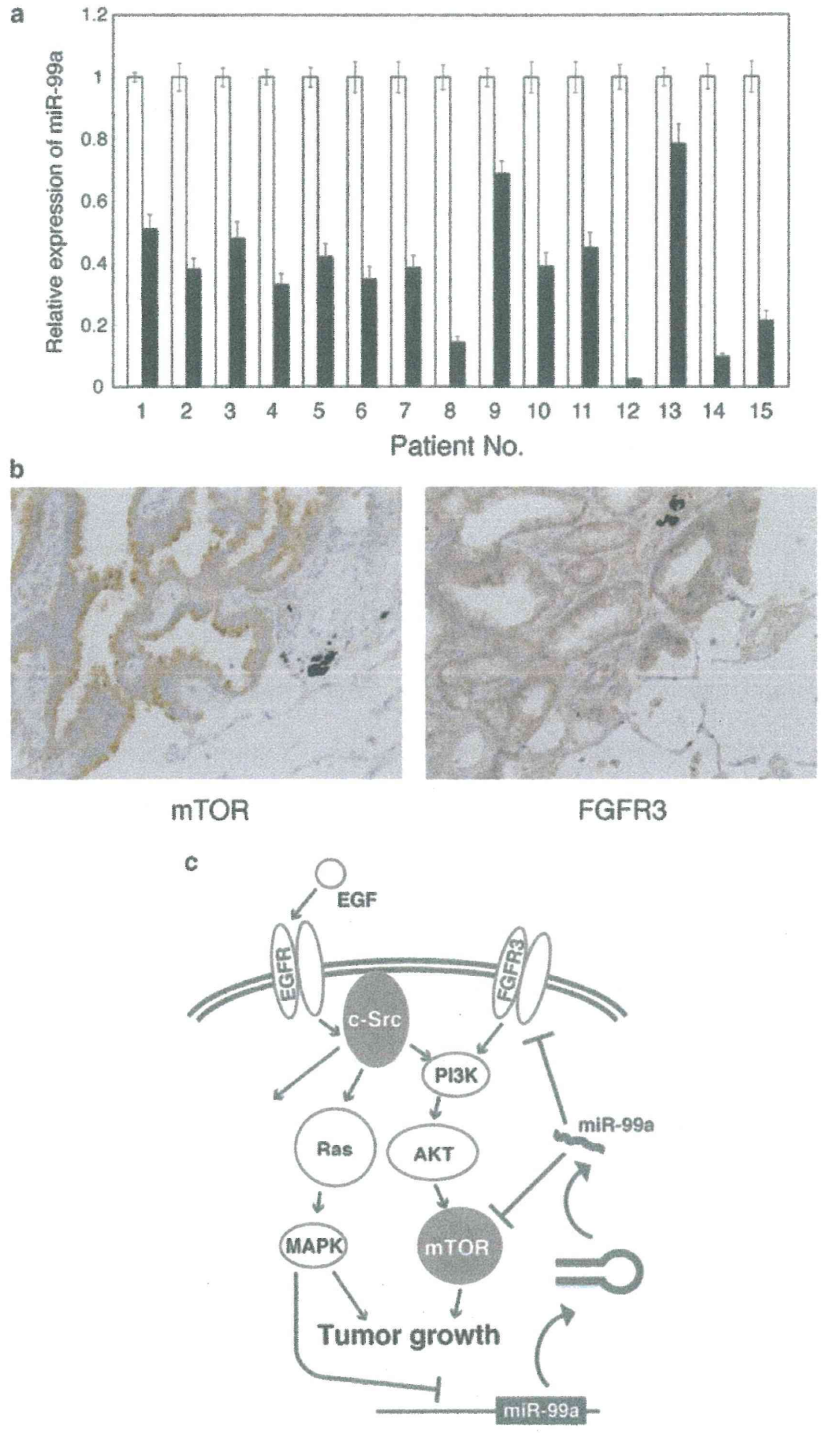

Figure 7 miR-99a in lung cancer tissues. (**a**) The expression of miR-99a in human lung tumors (black) and the corresponding normal tissue (white) from individual patients (1–15) was analyzed by qRT–PCR. Relative values ± s.d. were obtained from three independent assays. (**b**) Immunohistochemistry for mTOR and FGFR3 in lung adenocarcinoma and normal lung tissue samples (×400). Representative images from five samples are shown. (**c**) A schematic model of the function of miR-99a. The downregulation of miR-99a mediated by the Src-related oncogenic pathway results in the upregulation of mTOR and FGFR3, which in turn activates protein synthesis and the PI3K pathway, respectively, leading to the promotion of cell growth and survival.

system to study the potential role of miRNAs in c-Src-mediated tumor growth. The miRNA profiling identified seven miRNAs that were downregulated by c-Src transformation. A previous study showed that the expression of nine of 95 miRNAs that had been implicated in cancer, development and apoptosis was

affected by v-Src transformation (Li *et al.*, 2009). More recently, it was shown that 29 miRNAs were differentially expressed during transformation of MCF10A-ER-Src cells (Iliopoulos *et al.*, 2010). However, the miRNA species identified in the previous studies, such as miR-126, -218, -224, -21 or -181b-1 relevant to Src signaling and cancer, are not necessarily consistent with those identified in this study. Although the actual reasons are currently unclear, this inconsistency might be due to the difference in the pathways activated by v-Src and c-Src, or related to the cellular context. Because upregulation of c-Src protein and/or activity, rather than gain-of-function mutations in the *c-src* gene, widely contributes to the progression of human cancers, c-Src-transformed cells were used to identify miRNAs crucial for regulating human cancers.

Of the miRNAs downregulated by c-Src activation, we first focused on miR-99a, because recent reports suggested a potential tumor suppressor function of this miRNA in various human cancers (Yamada *et al.*, 2008; Doghman *et al.*, 2010; Gao *et al.*, 2010). We showed that it targets mTOR and FGFR3, both of which have been implicated in human cancers (Eswarakumar *et al.*, 2005; Guertin and Sabatini, 2007). A more recent study also showed that miR-99a can target the IGF-IR-mTOR-raptor pathway in a specific subset of human cancers (Doghman *et al.*, 2010), suggesting a role for miR-99a in regulating the oncogenic function of mTOR. However, the functional link between miR-99a and cancer progression is unclear, and the mechanisms underlying the downregulation of miR-99a in cancers remains to be addressed. This study provides the first firm evidence for tumor suppressive role of miR-99a and suggests that the expression of miR-99a is regulated via the Src-related oncogenic pathways involving EGFR, c-Src, K/H-Ras and MEK/ERK. In addition, the first evidence that perturbation of mTOR protein levels can directly contribute to controlling tumor growth is presented. As the Src-related oncogenic pathway is frequently activated in various human cancers, the functional analysis of the miR-99a–mTOR/FGFR3 axis driven by the EGFR/Src/Ras/MAPK pathway represents a great leap forward in our understanding of cancer etiology. Indeed, various human cancer cells, which harbor deregulation of c-Src, EGFR, K-Ras or N-myc, were shown to exhibit downregulation of miR-99a and upregulation of mTOR/FGFR3. The inhibition of mTOR function or introduction of miR-99a successfully suppressed tumor growth in certain types of human cancer cells. Furthermore, the existence of an inverse correlation between miR-99a and mTOR/FGFR3 in primary human cancer tissues was shown. Considering the crucial role of mTOR in various cancers, these observations support our proposal that the Src pathway–miR-99a–mTOR/FGFR3 axis is important in controlling tumor growth in a wide array of human cancers.

The substantial downregulation of miR-99a in human lung tumors suggests a crucial role for miR-99a as a regulator of these cancers. The *miR-99a* gene is located on chromosome 21q21.1, which was identified as a minimal region where loss of heterozygosity frequently occurs in cases of human lung cancer (Yamada *et al.*, 2008). The qRT–PCR analysis of miR-99a expression levels in a panel of lung cancer cell lines revealed a substantial reduction of miR-99a expression to less than one-tenth that of normal lung expression. To examine the possibility that these cell lines carry a homozygous deletion at 21q21.1, loss of heterozygosity analysis of A549 and PC10 cells was performed by genomic PCR, which confirmed that the 21q21.1 region is intact in these cells (data not shown). This observation suggests that activation of the Src/Ras-related oncogenic pathway, for example, *K-Ras* mutation, more widely contributes to the downregulation of miR-99a in cancer cells. However, downstream mechanisms that lead to changes in *miR-99a* gene expression remain unclear. Further extensive analysis will be necessary to elucidate the precise mechanism of miR-99a downregulation.

We also observed that ectopic expression of miR-99a suppressed anchorage-independent growth and tumorigenesis of c-Src-transformed cells, but it only moderately affected cell morphology. This could be attributed to the specific roles of mTOR and FGFR3 in regulating tumor growth and survival, respectively. On the basis of these findings, we propose a hypothetical model for the function of the miR-99a–mTOR/FGFR3 axis in tumor growth (Figure 7c). Downregulation of miR-99a caused by the activation of Src-related pathways results in the upregulation of mTOR and FGFR3, which in turn activate protein synthesis and the PI3K pathway, respectively, and promote tumor growth and survival. Earlier studies suggested that Src activity plays a critical role in the deregulation of mTOR signaling pathways, but the functional link between Src and mTOR was unclear (Penuel and Martin, 1999; Vojtechova *et al.*, 2008). It was also seen that mTOR is often overexpressed and activated in a wide variety of human cancers (Hay, 2005; Sabatini, 2006; Nozawa *et al.*, 2007); however, the underlying mechanisms remained unknown. This model for miR-99a function would provide a missing link between Src, mTOR and cancer progression.

The potential role of miRNA in mTOR regulation has previously been shown in studies of miR-100, an miRNA that contains the same seed sequences as miR-99a. It has been reported that miR-100 is downregulated in human cytomegalovirus infection and that re-expression of miR-100 reduces mTOR protein levels (Wang *et al.*, 2008). In addition, miR-100 is downregulated in clear cell ovarian cancer (Nagaraja *et al.*, 2010) and childhood adrenocortical tumors (Doghman *et al.*, 2010), and the overexpression of miR-100 inhibits mTOR signaling and enhances sensitivity to a mTOR inhibitor RAD001 (Nagaraja *et al.*, 2010). More recently, miR-199a-3p was also shown to be downregulated and target mTOR in hepatocarcinoma cells (Fornari *et al.*, 2010). These features of miR-100 and miR-199a-3p are quite similar to those of miR-99a, suggesting that mTOR expression might be regulated redundantly by these closely related miRNAs. However, downregulation of miR-100 and miR-199a-3p in c-Src-

transformed cells could not be detected (data not shown); this indicates that the expression of miR-100 and miR-199a-3p may be regulated through a pathway independent of the Src-related pathway or in different cellular contexts. Nonetheless, these findings strongly highlight a critical role of miRNA-mediated regulation of mTOR signaling in controlling tumor growth in various human cancers.

In conclusion, we have shown a crucial role for the Src–miR-99a–mTOR/FGFR3 axis in controlling tumor growth. Our study provides insights into the function of this new signaling axis, and offers new opportunities for therapeutic intervention in a wide array of human cancers.

Materials and methods

Pre-miR-99a and anti-miR-99a transfection
miR-99a precursor (PM10719), antisense miR-99a (AM11465) and control miR (AM17110) were purchased from Applied Biosystems (Foster City, CA, USA). The day before transfection, 2.5×10^5 cells were seeded onto six-well plates. Different concentrations of precursors (0.3–30 nM) and inhibitors (3–30 nM), as well as the negative control, were transfected using Lipofectamine RNAiMAX in 16 μl per six-well plates according to the manufacturer's instructions (Invitrogen, Carlsbad, CA, USA). Using this approach, 90% of cells were transfected as judged by comparison to FAM-labeled controls (AM17121; Applied Biosystems).

Soft-Agar colony formation assay
Single-cell suspensions of 2×10^4 cells were plated in six-well culture dishes in 1.5 ml of Dulbecco's modified Eagle's medium containing 10% fetal calf serum and 0.36% agar on a layer of 2.5 ml of the same medium containing 0.7% agar. Colonies were stained with 3-(4,5-dimethylthiazol-2-yl)- 2,5-diphenyltetrazolium bromide (Sigma, St Louis, MO, USA) 7–14 days after plating, and micrographs of the stained colonies were used to count the numbers of colonies.

Tumorigenesis assays
Immunodeficient mice (BALB/c AJcl-nu/nu; Japan CLEA, Tokyo, Japan) were injected subcutaneously with 1×10^6 cells suspended in 200 μl of serum-free Dulbecco's modified Eagle's medium at one location. Tumors were monitored every 2 or 3 days and the tumor volume was estimated using the following formula: $0.5 \times L \times W^2$. At least three mice were used in each experiment. The mice used for this study were handled in strict adherence with local governmental and institutional animal care regulations.

Immunohistochemistry
Histological specimens were fixed in 10% formalin and routinely processed for paraffin embedding. Histological sections 4-μm thick were stained with hematoxylin and eosin and reviewed by two pathologists (JI and EM) to define the cancerous and corresponding normal tissues. An immunoperoxidase procedure was performed on the paraffin-embedded sections as described below. After antigen retrieval using a Pascal pressurized heating chamber (Dako A/S, Glostrup, Denmark), the sections were incubated with anti-mTOR or anti-FGFR3 antibody that was diluted at 1:50. Cells were then treated with a ChemMate EnVision kit (Dako). Diaminobenzidine (Dako) was used as a chromogen. As a negative control, staining was carried out in the absence of primary antibody. Stained sections were evaluated independently by two pathologists (JI and EM).

Conflict of interest

The authors declare no conflicts of interest.

Acknowledgements

We thank Drs A Imamoto, T Akagi and M Yutsudo for generous gifts of reagents. This work was supported by a Grant-in-aid for Young Scientists from the Ministry of Education, Culture, Sports, Science and Technology of Japan and The Exciting Leading-Edge Research Project at Osaka University.

References

Ambros V. (2004). The functions of animal microRNAs. *Nature* **431**: 350–355.
Bartel DP. (2004). MicroRNAs: genomics, biogenesis, mechanism, and function. *Cell* **116**: 281–297.
Bartel DP. (2009). MicroRNAs: target recognition and regulatory functions. *Cell* **136**: 215–233.
Brown M, Cooper J. (1996). Regulation, substrates and functions of src. *Biochim Biophys Acta* **1287**: 121–149.
Calin GA, Croce CM. (2006). MicroRNA signatures in human cancers. *Nat Rev Cancer* **6**: 857–866.
Catto JW, Miah S, Owen HC, Bryant H, Myers K, Dudziec E *et al.* (2009). Distinct microRNA alterations characterize high- and low-grade bladder cancer. *Cancer Res* **69**: 8472–8481.
Doghman M, El Wakil A, Cardinaud B, Thomas E, Wang J, Zhao W *et al.* (2010). Regulation of insulin-like growth factor-mammalian target of rapamycin signaling by microRNA in childhood adrenocortical tumors. *Cancer Res* **70**: 4666–4675.
Engelman JA. (2009). Targeting PI3K signalling in cancer: opportunities, challenges and limitations. *Nat Rev Cancer* **9**: 550–562.
Esquela-Kerscher A, Slack FJ. (2006). Oncomirs—microRNAs with a role in cancer. *Nat Rev Cancer* **6**: 259–269.
Eswarakumar VP, Lax I, Schlessinger J. (2005). Cellular signaling by fibroblast growth factor receptors. *Cytokine Growth Factor Rev* **16**: 139–149.
Fornari F, Milazzo M, Chieco P, Negrini M, Calin GA, Grazi GL *et al.* (2010). MiR-199a-3p regulates mTOR and c-Met to influence the doxorubicin sensitivity of human hepatocarcinoma cells. *Cancer Res* **70**: 5184–5193.
Frame M. (2002). Src in cancer: deregulation and consequences for cell behaviour. *Biochim Biophys Acta* **1602**: 114–130.
Gao W, Shen H, Liu L, Xu J, Shu Y. (2010). MiR-21 overexpression in human primary squamous cell lung carcinoma is associated with poor patient prognosis. *J Cancer Res Clin Oncol* (e-pub ahead of print 17 February 2011; DOI:10.1007/s00432-011-0976-2).
Guertin DA, Sabatini DM. (2007). Defining the role of mTOR in cancer. *Cancer Cell* **12**: 9–22.
Hakak Y, Martin GS. (1999). Ubiquitin-dependent degradation of active Src. *Curr Biol* **9**: 1039–1042.
Hay N. (2005). The Akt-mTOR tango and its relevance to cancer. *Cancer Cell* **8**: 179–183.
Hay N, Sonenberg N. (2004). Upstream and downstream of mTOR. *Genes Dev* **18**: 1926–1945.
He L, Hannon GJ. (2004). MicroRNAs: small RNAs with a big role in gene regulation. *Nat Rev* **5**: 522–531.

Iliopoulos D, Jaeger SA, Hirsch HA, Bulyk ML, Struhl K. (2010). STAT3 activation of miR-21 and miR-181b-1 via PTEN and CYLD are part of the epigenetic switch linking inflammation to cancer. *Mol Cell* **39**: 493–506.

Ingley E. (2008). Src family kinases: regulation of their activities, levels and identification of new pathways. *Biochim Biophys Acta* **1784**: 56–65.

Irby R, Mao W, Coppola D, Kang J, Loubeau J, Trudeau W *et al.* (1999). Activating SRC mutation in a subset of advanced human colon cancers. *Nat Genet* **21**: 187–190.

Irby R, Yeatman T. (2000). Role of Src expression and activation in human cancer. *Oncogene* **19**: 5636–5642.

Ishizawar R, Parsons S. (2004). c-Src and cooperating partners in human cancer. *Cancer Cell* **6**: 209–214.

Li X, Shen Y, Ichikawa H, Antes T, Goldberg GS. (2009). Regulation of miRNA expression by Src and contact normalization: effects on nonanchored cell growth and migration. *Oncogene* **28**: 4272–4283.

Liu P, Cheng H, Roberts TM, Zhao JJ. (2009). Targeting the phosphoinositide 3-kinase pathway in cancer. *Nat Rev Drug Discov* **8**: 627–644.

Menon S, Manning BD. (2008). Common corruption of the mTOR signaling network in human tumors. *Oncogene* **27**(Suppl 2): S43–S51.

Nada S, Okada M, MacAuley A, Cooper JA, Nakagawa H. (1991). Cloning of a complementary DNA for a protein-tyrosine kinase that specifically phosphorylates a negative regulatory site of p60c-src. *Nature* **351**: 69–72.

Nagaraja AK, Creighton CJ, Yu Z, Zhu H, Gunaratne PH, Reid JG *et al.* (2010). A link between mir-100 and FRAP1/mTOR in clear cell ovarian cancer. *Mol Endocrinol* **24**: 447–463.

Nagayama K, Kohno T, Sato M, Arai Y, Minna JD, Yokota J. (2007). Homozygous deletion scanning of the lung cancer genome at a 100-kb resolution. *Genes Chromosomes Cancer* **46**: 1000–1010.

Nam EJ, Yoon H, Kim SW, Kim H, Kim YT, Kim JH *et al.* (2008). MicroRNA expression profiles in serous ovarian carcinoma. *Clin Cancer Res* **14**: 2690–2695.

Noro R, Gemma A, Kosaihira S, Kokubo Y, Chen M, Seike M *et al.* (2006). Gefitinib (IRESSA) sensitive lung cancer cell lines show phosphorylation of Akt without ligand stimulation. *BMC Cancer* **6**: 277.

Nozawa H, Watanabe T, Nagawa H. (2007). Phosphorylation of ribosomal p70 S6 kinase and rapamycin sensitivity in human colorectal cancer. *Cancer Lett* **251**: 105–113.

Okada M, Nada S, Yamanashi Y, Yamamoto T, Nakagawa H. (1991). CSK: a protein-tyrosine kinase involved in regulation of src family kinases. *J Biol Chem* **266**: 24249–24252.

Oneyama C, Hikita T, Nada S, Okada M. (2008). Functional dissection of transformation by c-Src and v-Src. *Genes Cells* **13**: 1–12.

Ong SH, Hadari YR, Gotoh N, Guy GR, Schlessinger J, Lax I. (2001). Stimulation of phosphatidylinositol 3-kinase by fibroblast growth factor receptors is mediated by coordinated recruitment of multiple docking proteins. *Proc Natl Acad Sci USA* **98**: 6074–6079.

Penuel E, Martin G. (1999). Transformation by v-Src: Ras-MAPK and PI3K-mTOR mediate parallel pathways. *Mol Biol Cell* **10**: 1693–1703.

Petroulakis E, Mamane Y, Le Bacquer O, Shahbazian D, Sonenberg N. (2006). mTOR signaling: implications for cancer and anticancer therapy. *Br J Cancer* **94**: 195–199.

Sabatini DM. (2006). mTOR and cancer: insights into a complex relationship. *Nat Rev Cancer* **6**: 729–734.

Shenouda SK, Alahari SK. (2009). MicroRNA function in cancer: oncogene or a tumor suppressor? *Cancer Metast Rev* **28**: 369–378.

Trudel S, Ely S, Farooqi Y, Affer M, Robbiani DF, Chesi M *et al.* (2004). Inhibition of fibroblast growth factor receptor 3 induces differentiation and apoptosis in t(4;14) myeloma. *Blood* **103**: 3521–3528.

van Rhijn BW, Lurkin I, Radvanyi F, Kirkels WJ, van der Kwast TH, Zwarthoff EC. (2001). The fibroblast growth factor receptor 3 (FGFR3) mutation is a strong indicator of superficial bladder cancer with low recurrence rate. *Cancer Res* **61**: 1265–1268.

Ventura A, Jacks T. (2009). MicroRNAs and cancer: short RNAs go a long way. *Cell* **136**: 586–591.

Vojtechova M, Tureckova J, Kucerova D, Sloncova E, Vachtenheim J, Tuhackova Z. (2008). Regulation of mTORC1 signaling by Src kinase activity is Akt1-independent in RSV-transformed cells. *Neoplasia* **10**: 99–107.

Wang FZ, Weber F, Croce C, Liu CG, Liao X, Pellett PE. (2008). Human cytomegalovirus infection alters the expression of cellular microRNA species that affect its replication. *J Virol* **82**: 9065–9074.

Wong TS, Liu XB, Wong BY, Ng RW, Yuen AP, Wei WI. (2008). Mature miR-184 as potential oncogenic microRNA of squamous cell carcinoma of tongue. *Clin Cancer Res* **14**: 2588–2592.

Wullschleger S, Loewith R, Hall MN. (2006). TOR signaling in growth and metabolism. *Cell* **124**: 471–484.

Yamada H, Yanagisawa K, Tokumaru S, Taguchi A, Nimura Y, Osada H *et al.* (2008). Detailed characterization of a homozygously deleted region corresponding to a candidate tumor suppressor locus at 21q11–21 in human lung cancer. *Genes Chromosomes Cancer* **47**: 810–818.

Yeatman TJ. (2004). A renaissance for SRC. *Nat Rev Cancer* **4**: 470–480.

Yokota J, Kohno T. (2004). Molecular footprints of human lung cancer progression. *Cancer Sci* **95**: 197–204.

Supplementary Information accompanies the paper on the Oncogene website (http://www.nature.com/onc)

ELSEVIER

European Journal of Cardio-thoracic Surgery 40 (2011) 322–327

EUROPEAN JOURNAL OF CARDIO-THORACIC SURGERY

www.elsevier.com/locate/ejcts

Winner of the EACTS Young Investigator Award 2010 - Category 'Thoracic'.

Novel approach for detection of isolated tumor cells in pulmonary vein using negative selection method: morphological classification and clinical implications☆,☆☆

Soichiro Funaki, Noriyoshi Sawabata*, Tomoyuki Nakagiri, Yasushi Shintani, Masayoshi Inoue, Yoshiki Kadota, Masato Minami, Meinoshin Okumura

Department of General Thoracic Surgery, Osaka University Graduate School of Medicine, Osaka, Japan

Received 10 August 2010; received in revised form 28 October 2010; accepted 4 November 2010; Available online 7 January 2011

Abstract

Objective: The presence of isolated tumor cells (ITCs) in the pulmonary vein (PV) of a lung resected for lung cancer has been reported to be a prognostic factor. Previous investigations noted correlations between prognosis and the presence or amount of ITCs, although few studies have investigated the clinical implications of the morphological characteristics of those cells. We assessed the clinical implications of ITCs in the PV using a novel enrichment approach that maintained their morphological characteristics. **Methods:** Ninety-four consecutive patients with primary non-small-cell lung cancer (NSCLC) without preoperative chemo- and/or radiation therapy (p-stage I in 75, II in 13, III or IV in six) were studied. Blood samples were drawn from the PV draining the lung just after pulmonary resection, and ITCs were enriched using a CD45-negative selection method and density-gradient centrifugation, followed by Papanicolaou staining using 1 ml of PV blood and immunohistochemical staining for cytokeratin in cases with an additional available blood sample. The ITCs were classified into four types based on patterns of cluster formation: no tumor cells (N), singular tumor cells (S), clustered cells ($\leq$0.2 mm) (CSs), and bulky clustered cells (>0.2 mm) (BCSs). We evaluated the correlations between ITC morphology and clinical results. **Results:** ITCs were detected in 68 of 94 patients (72%), of which the BCS type was observed in two, CS in 33, S in 33, and N in 26. Over a median follow-up period of 13 months (range 6–22 months), cancer recurrence occurred in 16 cases (17%): 14 in the combined CS/BCS group, one in S, and one in N. Log-rank analysis revealed that the disease-free survival rate was exclusively worse in patients with clustered ITCs as compared with the other two groups ($p < 0.01$). **Conclusions:** The present method was useful to detect and enrich ITCs from the PV, and showed the clinical relevance of their morphology in lung cancer cases. The presence of ITC clusters may be a prognostic biomarker for patients with resected NSCLC.

Keywords: Lung cancer; Surgery; Isolated tumor cells; Morphology

1. Introduction

Primary lung cancer remains a leading cause of cancer death in most industrialized countries [1], with most cancer deaths related to high rates of recurrence and distant metastasis; thus, useful biomarkers are needed for early detection of both. Recently, isolated tumor cells (ITCs) in blood were reported to be useful markers for prognosis, recurrence, and metastasis [2]. It has been speculated that ITCs are likely shed from the primary tumor, then flow through a drainage vein and circulate throughout the body.

A number of methods to detect ITCs have been reported, with polymerase chain reaction (PCR)-based assays the most widely used [3], as a high sensitivity of ITC detection and clinical implications of the results have been shown [4–6]. Recently, the CellSearch® System (Veridex LLC, Rartian, NJ, USA) was shown to provide accurate detection and enrichment of rare ITCs from blood samples of patients with various types of solid cancer, including lung cancer [7], colon cancer [8], and breast cancer at the single cell level [9]. In addition,

☆ Presented at the 24th Annual Meeting of the European Association for Cardio-thoracic Surgery, Geneva, Switzerland, September 11–15, 2010.

☆☆ This research was supported by a Grant-in-Aid for Scientific Research (B) from the Japan Ministry of Education, Science, Sports and Culture, and the Uehara Memorial Foundation.

* Corresponding author. Address: Department of General Thoracic Surgery, Osaka University Graduate School of Medicine, L-5 2-2 Yamadaoka Suita-city, Osaka, 565-0897, Japan. Tel.: +81 6 6879 3152; fax: +81 6 857 3179.

E-mail addresses: sawabata@thoracic.med.osaka-u.ac.jp, nsawabata@hotmail.com (N. Sawabata).

1010-7940/$ – see front matter
doi:10.1016/j.ejcts.2010.11.029

associations between the number of ITCs with tumor stage and progression have been reported [10]. Most previous studies were quantitative investigations used to evaluate ITCs, and there are few reports of the clinical implication of ITCs that used morphological classification. We conducted the present investigation to assess the clinical implications and morphological characteristics of ITCs in the PV of resected lungs of non-small-cell lung cancer (NSCLC) patients using a novel approach for ITC enrichment and detection.

2. Patients and methods

2.1. Cell-spiking experiment

Initially, to evaluate the accuracy and sensitivity of our method to detect ITCs, a cell-spiking experiment was performed using two lung cancer cell lines, COR-L32 (human small-cell lung carcinoma; ATCC® Catalogue No. 96020744) and SK-LU-1 (human adenocarcinoma; ATCC® Catalogue No. HTB-57™), prior to the examination of clinical samples to detect ITCs in blood samples. The cell lines were maintained in Eagle's Minimum Essential Medium (EMEM) supplemented with fetal bovine serum (FBS) to a final concentration of 10% and incubated at 37 °C. After adding a known number of cells to 1-ml whole blood samples obtained from healthy volunteers, we assessed the sensitivity of our method by determining the ratio of the number of enriched cells to the number of added cells with a hemacytometer.

The method of cell extraction employed was as follows. A RosetteSep® Human CD45 Depletion Cocktail (Stemcell Technologies, Inc.) was added at 50 μl ml^{-1} to individual whole blood samples and mixed well. After incubation for 20 min at room temperature, the mixture was diluted with an equal volume of phosphate-buffered saline + 2% fetal bovine serum (PBS + 2% FBS) and mixed gently. The diluted sample was then layered on top of a Ficoll-Paque™ PLUS and centrifuged for 20 min at 1200 $\times$ g at room temperature, with the brake in the off position; then, the enriched ITCs were removed from the Ficoll-Paque™ PLUS–plasma interface. After washing enriched ITCs with PBS + 2% FBS, the cells were centrifuged down to polylysine-coated glass slides using a cytospin device at 1000 $\times$ g for 3 min. Cells on the slides were stained using Papanicolaou stain and a cytokeratin immunohistochemistry kit (Carcinoma cell detection kit human, Miltenyi Biotec® Catalogue No. 130-090-463), which resulted in a cell collection ratio of 60% for both single cells and clustered cells. Tumor cells that existed among the total nuclear cell count ranged from 1×10^2 to 1×10^3 in number.

Table 1. Patient characteristics and distribution of isolated tumor cells in pulmonary venous blood.

	Total	PV cytology			*p*-Value
		N	S	C	
No.	94	26	33	35	
Gender					0.8
Male	56	17	19	20	
Female	38	9	14	15	
Age (mean ± SD)	67.7 ± 8.4	68.8 ± 8.3	67.2 ± 9.0	70.0 ± 10.9	0.5
<70	49	14	21	14	0.1
≥70	45	12	12	21	
pT factor					0.3
T1	52	18	19	15	
T2	36	7	12	17	
T3	6	1	2	3	
pN factor					1.0
N0	84	24	29	31	
N1	4	1	2	1	
N2	5	1	2	2	
NX	1	0	0	1	
pM factor					1.0
M0	93	26	33	34	
M1a	1	0	0	1	
M1b	0	0	0	0	
p-Stage					0.6
I	75	23	27	25	
II	13	2	4	7	
III or IV	6	1	2	3	
Tumor histology					0.9
Adenocarcinoma	71	19	26	26	
Squamous cell carcinoma	14	4	5	5	
Miscellaneous	9	3	2	4	
Tumor location					0.1
RU	44	13	13	18	
RM	3	0	3	0	
RL	13	2	6	5	
LU	23	4	9	10	
LL	11	7	2	2	

PV, pulmonary vein; N, no tumor cells; S, singular tumor cells; CS/BCS, clustered tumor cells; RU, right upper lobe; RM, right middle lobe; RL, right lower lobe; LU, left upper lobe; LL, left lower lobe.